

COMPUTATIONAL ANALYSIS OF NATURAL CONVECTION IN ASYMMETRICALLY HEATED INCLINED OPEN-ENDED CHANNELS WITH VERY LOW INTERWALL SPACING

Several computational simulations were performed for simulating natural convection in open-ended inclined parallel-walled channels. Variations in the thermophysical parameters such as interwall spacing S , angle of inclination with vertical θ and wall-ambience temperature difference ΔT were considered. The Nusselt number shows a positive correlation with the $\sin \theta$ at very low interwall spacing ($S < 0.01\text{m}$) and a change in positive correlation from the sine to the cosine at higher interwall spacings ($S \sim 0.025\text{m}$). The simulations also indicate a sudden increase in the Nusselt number at higher angle of inclinations with the vertical at very low aspect ratios (S/H). A generalized correlation $Nu_S = 0.6635[(S/H) Ra_S \sin \theta]^{1/3}$ represents results for channels with aspect ratios < 0.01 within $\pm 10\%$. Flow recirculation was observed close to the unheated walls.

NOMENCLATURE

S	= interwall Spacing, Figure 1
H	= length of the channel along the primary direction of flow, Figure 1
W	= width of the channel across the primary direction of flow, Figure 1
θ	= angle of inclination of the channel with the vertical, Figure 2
g	= acceleration due to gravity
β	= coefficient of thermal expansion
k	= thermal conductivity
ν	= kinematic viscosity
ρ	= density
Ra_S	= Rayleigh number, Equations (1), (2), (3)
Gr_S	= Grashof number
Pr	= Prandtl number
Nu_S	= surface Nusselt number
Q_S	= heat transfer rate from surface
ΔT	= temperature difference between surface and ambience

INTRODUCTION

Laminar natural convection in open-ended parallel plate inclined channels and the effects of various geometric and flow parameters have been extensively researched over the years, extending to several variations in the flow setup such as asymmetry in heating. The Nusselt number of the flow has been experimentally correlated with parameters like the Rayleigh number of the flow, the aspect ratio of flow regime and the angle of inclination, with the Nusselt number exhibiting a direct correlation with the cosine of the angle of inclination with the vertical. However, there is relatively little research on the phenomenon at higher aspect ratios and smaller interwall spacings during asymmetric heating. The objective of this paper is to present a report on the phenomenon at such geometrical and thermal conditions. The

presented research is of significance to estimating and modelling the heat transfer and flow properties in applications like natural convection driven panel based liquid cooling systems.

The primary focus of the research is to determine if there are variations in the existing correlations of the Nusselt number and geometric parameters like the interwall spacing, the angle of inclination with the vertical and the aspect ratio of the channel, at extreme values. Apart from the geometrical parameters of flow, thermal parameters like the input heat flux and the temperature gradient between the heated wall and the surroundings were also altered to determine their effects on the Nusselt number at said extreme conditions. In addition to the above parameters, various computational parameters and conditions were also tested to improve the computational accuracy of natural convection. The existing correlations were computationally verified before proceeding to the test case and a mesh sensitivity analysis was performed to ensure precision of the obtained results.

Currently, flat plate solar collectors are typically cooled by convection with air as the convective fluid medium. Natural convection in air is a very slow process and one which has a low heat transfer rate. The solar collectors, being highly inefficient at higher temperatures, require a more consistent and intensive cooling method to lower the surface temperature to optimal levels. Liquid cooling of the panels through natural convection induced flow is one of the possible ways to reduce the surface temperature. The existing correlations predict an error range of $\pm 10\%$ in determining the Nusselt number in geometrically extreme regimes. However, computational simulations suggest a variation in the correlations in such a case which can be attributed to two reasons – the interwall spacing is on very small orders of magnitude and the angle of inclination with vertical is very large, bordering on 90° . Although research has been conducted on such cases of extreme values of interwall spacings and inclination angles, a high fraction of the research considered air as the operating fluid. Since the setup in consideration involves a reinforcing operating fluid driven by natural convection from the solar panel, such correlations cannot be easily adapted to the current case.

Computational analysis of natural convection is susceptible to deviations from actual experimental results primarily because the flow is buoyancy driven and hence, density of the fluid varies with the temperature field. A conventional workaround involves approximating variation in density with temperature to a linear model forms the basis of most analysis of natural convection. However, in realistic cases, approximation of density variation with respect to temperature to a linear model holds good only for small temperature changes. Across larger temperature variations, the variation of density will depend on the thermal expansion coefficient which itself would be non-linear.

PROBLEM DESCRIPTION

The purpose of this research is to provide a footing on the behaviour of natural convection driven flows in very thin channels with a high angle of inclination with the vertical. This may find its application in liquid cooled flat plate photovoltaic solar panels. The heat outflux in a solar panel at peak temperature is very high and it subsequently heats up the surface of the panel. Photovoltaic solar panels are known to be highly inefficient at higher temperatures and hence, cooling down the surface and maintaining at an optimal temperature of 40° would be beneficial in increasing the power conversion rate. Conventionally, this is performed by means of a cooling channel driven by natural convection. A liquid medium with a high thermal

expansion coefficient and a low viscosity would better suit the case and can provide a higher heat transfer coefficient compared to a gaseous convective medium.

The setup of the simulation consists of an open channel inclined flow regime with the top wall kept unheated and adiabatic and the bottom wall serving as a heat influx wall, conditions which are typically seen in the cooling setup of a flat plate solar panel, as shown in the drawing below (Figure 1). Water was used as the operating fluid and optimal temperature differences between the panel and the inlet temperature of the fluid was taken and varied to determine its correlation. The angle of inclination with the vertical and the interwall spacing were altered in discrete steps with a new geometry created for each case.

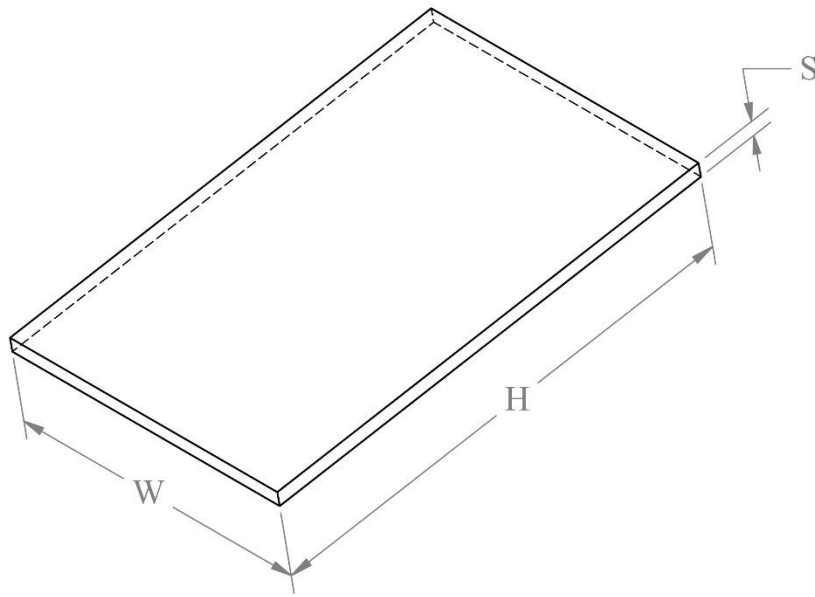


FIGURE 1: PROBLEM SETUP

The surface Nusselt number (Nu_S) is significant in determining the heat transfer coefficient of the flow, which in turn would be useful in determining the heat flux through convection and subsequently, the heat outflux through the hot surface. The correlation of Nusselt number is to be made against the Rayleigh number of the flow, the aspect ratio of the flow channel and the angle of inclination with the vertical. The Rayleigh number of the flow for a constant temperature gradient between the heated wall and the ambience can be described as follows:

$$Ra_S = Gr_S \cdot Pr \quad \dots (1)$$

$$Ra_S = \frac{g\beta\Delta TS^3}{\nu\alpha} \quad \dots (2)$$

$$Ra_S = \frac{g\beta Q_S S^4}{k\nu\alpha} \quad \dots (3)$$

The above equations describe different variations in the determination of the Rayleigh number based on the known parameters and conditions. Equation (1) is a general definition of the Rayleigh number as the product of the Grashof number of flow (Gr_S) and the Prandtl number

of the fluid medium (Pr). Equations (2) and (3) are merely a result of the expansions of the Grashof number and the Prandtl number as functions of fundamental thermophysical properties of flow such as the expansion coefficient (β), kinematic viscosity (ν) and the thermal diffusivity (α). Equation (2) is used when the heated wall is isothermal in nature and equation (3), when the heated wall is isoflux in nature.

The visualisation of the simulated flow indicates a developed flow along a majority of the length of the channels with a similar velocity profile throughout the channel except for the developing region. A characteristic feature of the flow profile is the reversed flow in the middle of the channel during flow development and subsequent reversal through development. The flow profile was monitored at different time steps through unsteady flow analysis.

PRE-PROCESSING OPERATIONS

The CFD simulations were performed in ANSYS Fluent. Before proceeding with the simulations, several pre-processing operations were performed to validate the accuracy of the results obtained from the simulations. Fluent is a capable CFD tool that has several inbuilt solver settings pertaining to natural convection driven flows such as Boussinesq approximation. The software also has features relevant to the case in hand i.e., tools such as estimation of surface Nusselt number and heat transfer coefficient. The software also supports an adequate mesh resolution enabling a sufficient resolution of the small interwall spacing. The ANSYS Meshing tool allows customising the resolution of mesh with a variety of options like local mesh resolution modifications and modification of parameters like the growth ratio, curvature, mesh cell types.

Flow Geometry

As the flow is quasi-one-directional flow with a secondary flow across the channel, the dimension of depth (Z-axis) is neglected for the simulations. Hence, a 2D flow regime was considered for the entirety of the analysis. Realistically, there will be a variation in the flow only along the edges of the cuboidal channel and this can be countered by extending the flow channel over the panel surface by a marginal length. This will prevent high temperature gradients at the edges of the panel and ensure a uniform undisrupted flow. A modification as stated above will also ensure there are no tertiary flows along the Z axis and hence, the flow regime for analysis can be effectively taken to be 2D, in the XY plane.

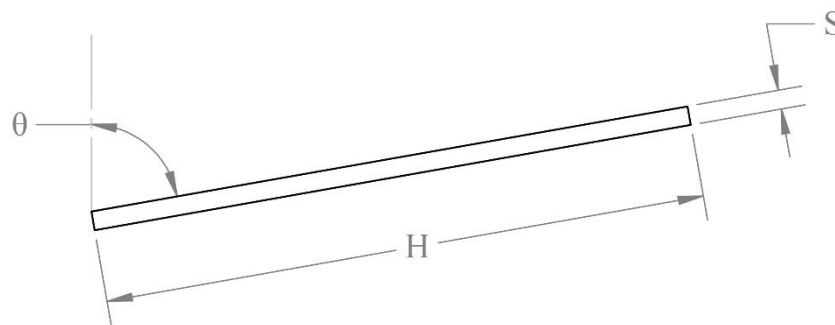


FIGURE 2: SIMULATION SETUP

Azevedo and Sparrow determined correlations for asymmetric natural convection driven flows in open ended inclined channels up to an aspect ratio of 0.0437, with an increasing tolerance level at lower values. However, as the convective medium is a liquid, radiation losses being predominant over that in a gaseous medium, the aspect ratio of the liquid cooling channel must be smaller. Effectively, a 1cm wide channel is to be taken as one of the extreme cases for this analysis, which leads us to an extreme value of the aspect ratio in the range 0.001, approximately 40 times smaller than previous literature.

In all of the simulations performed, the length of the channel (H) was kept at a constant value of 1m. The interwall spacing (S) and the angle of inclination (θ) with the vertical was changed with each simulation. The angle of inclination can be changed either by varying the flow geometry itself or by using a vector form for acceleration due to gravity and subsequently varying the values for the horizontal and vertical components directly in the solver. However, the former method was taken to ensure similar solver settings throughout the simulations. The range of the aspect ratios taken for simulation were [0.008, 0.025], with the angle of inclination varying from 15° to 75° . Usually, solar panels have an optimal mean tilt angle with respect to the vertical of 10° to 45° depending on the latitude. Hence, the fluid flow channel will be inclined at the same angle, parallel to the panel.

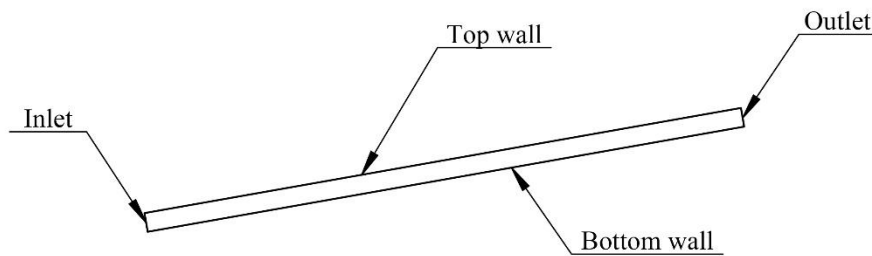


FIGURE 3: FLOW GEOMETRY

There are four boundaries on the flow geometry – the bottom wall, the top wall, the inlet and the outlet. Since convection is the only mode of heat transfer in focus, conduction across the wall and other parameters pertaining to the material of the wall is irrelevant. Hence, the walls are of negligible thickness and are one-dimensional. The walls exist only as boundaries for the fluid flow and do not constitute an individual part of the solution.

Meshing

The ANSYS Meshing program was used to create a mesh of the flow regime. A triangular mesh definition was used. As the flow along the thin channel is to be closely monitored, a detailed resolution across the interwall spacing is required. The channel spacing (S) and the length (H) were defeatured into elements of cell length 0.5 mm, resulting from 16 to 50 nodes along the interwall spacing depending on the geometry used. Through mesh defeaturing, the adjacent cells to a wall effectively defeature the walls further in half, to a size of 0.25 mm.

The specifications of the mesh along with parameters pertaining to the quality of the mesh are detailed in the table below.

S. NO.	PARAMETER	VALUE
1	Element Size	5 e-4 m
2	Growth Rate	1.2
3	Mesh Defeature Size	2.5 e-4 m
4	Nodes	~34000
5	Elements	~64000
6	Minimum Cell Aspect Ratio	~ 1
7	Maximum Cell Aspect Ratio	~ 2.6
8	Average Cell Aspect Ratio	~ 1.3
9	Minimum Skewness	~ 1 e-5
10	Maximum Skewness	~ 0.64
11	Average Skewness	~ 0.1
12	Minimum Orthogonal Quality	~ 0.62
13	Maximum Orthogonal Quality	~ 1
14	Average Orthogonal Quality	~ 0.94

TABLE 1: MESH SPECIFICATIONS

It can be seen that the orthogonal quality of the mesh is in tolerance with the acceptable thumb rule of > 0.3 . The cells possessing worse orthogonal quality or skewness is very few in number as illustrated by figures. A section of the mesh is also illustrated below in the figure to portray the mesh resolution across the interwall spacing.

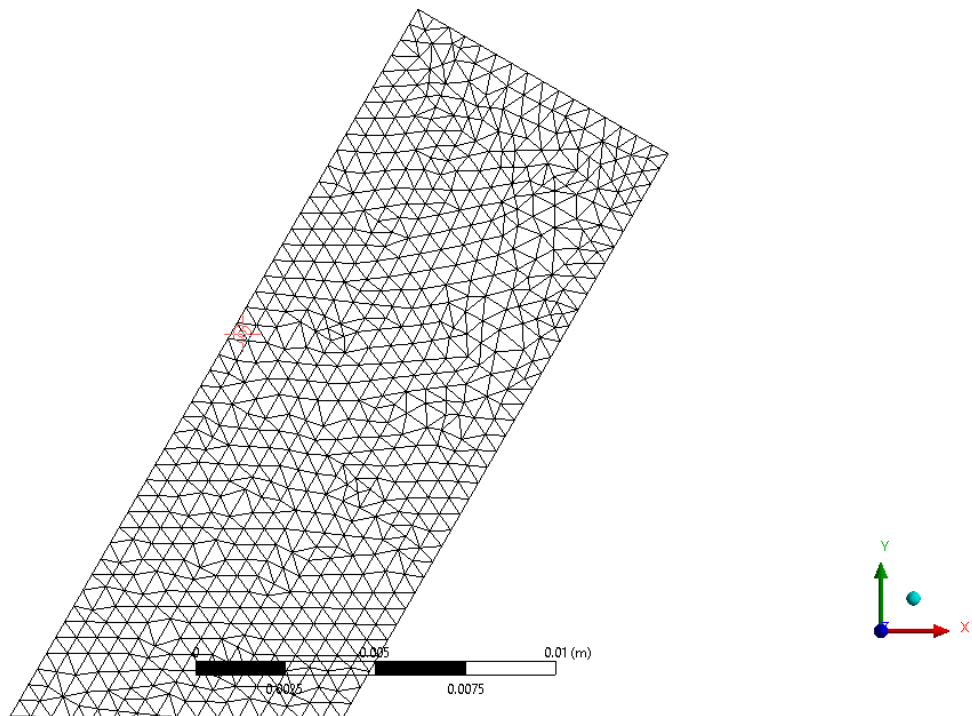


FIGURE 4: MESH RESOLUTION

The following figures describe the distribution of various qualitative parameters – cell corner angle, cell aspect ratio, skewness and orthogonal quality across the mesh.

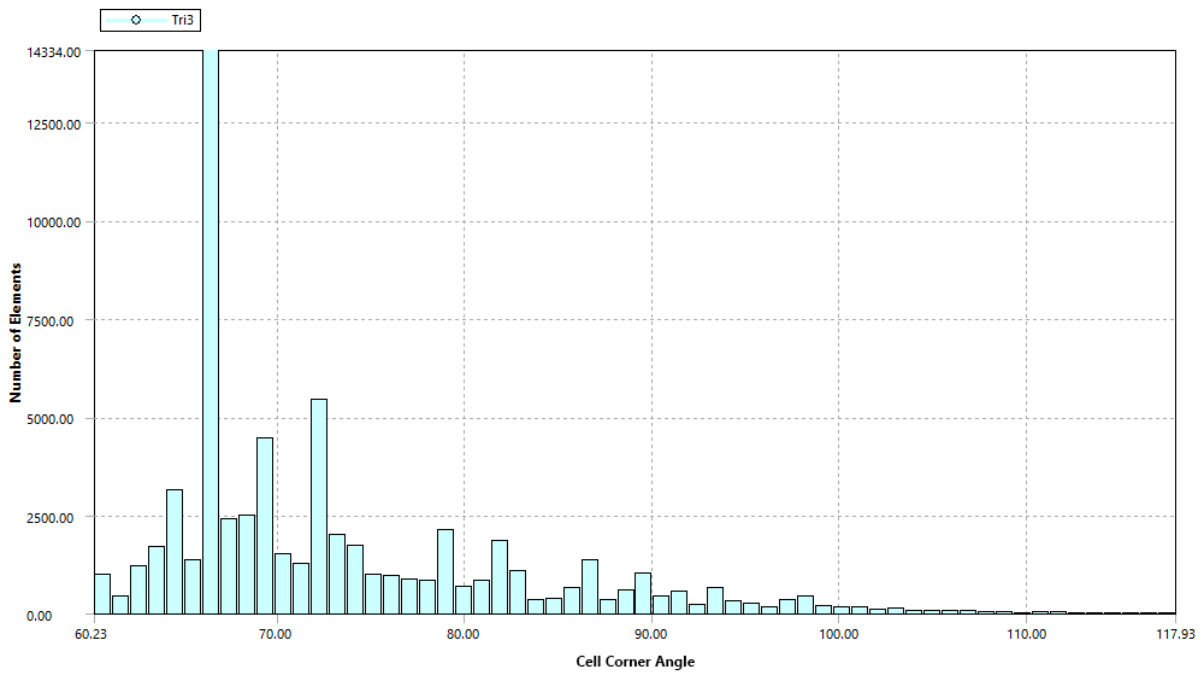


FIGURE 5: DISTRIBUTION OF CELL CORNER ANGLE

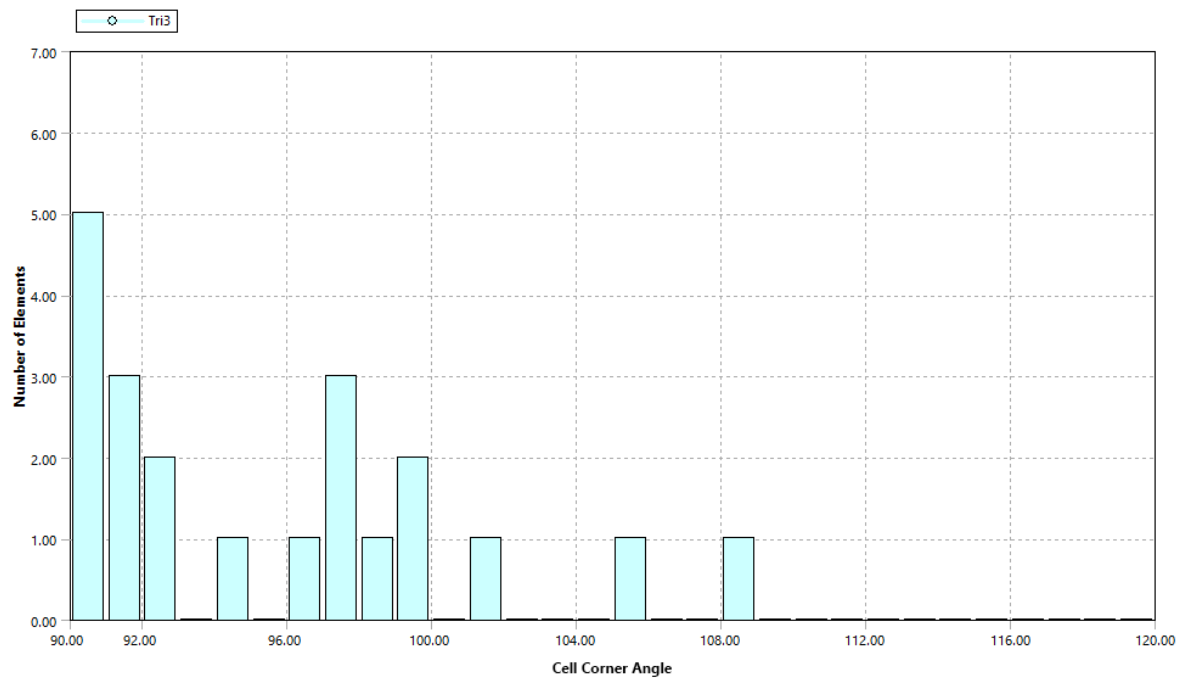


FIGURE 6: DISTRIBUTION OF OBTUSE ANGLES IN MESH

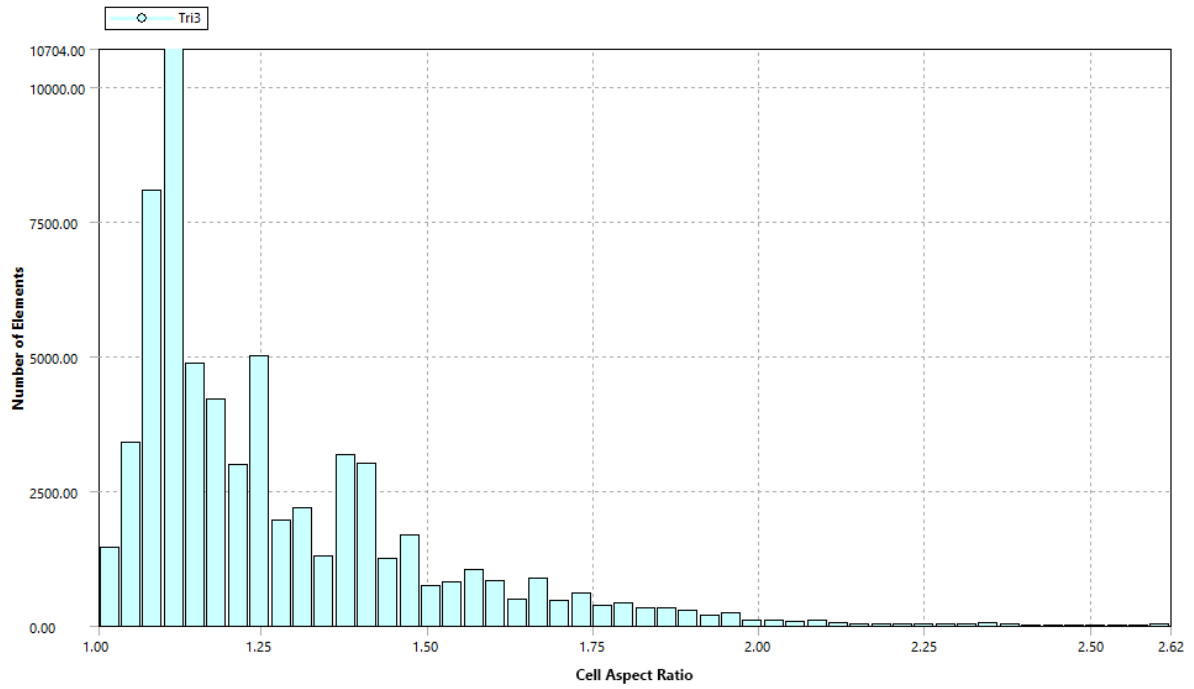


FIGURE 7: DISTRIBUTION OF CELL ASPECT RATIO

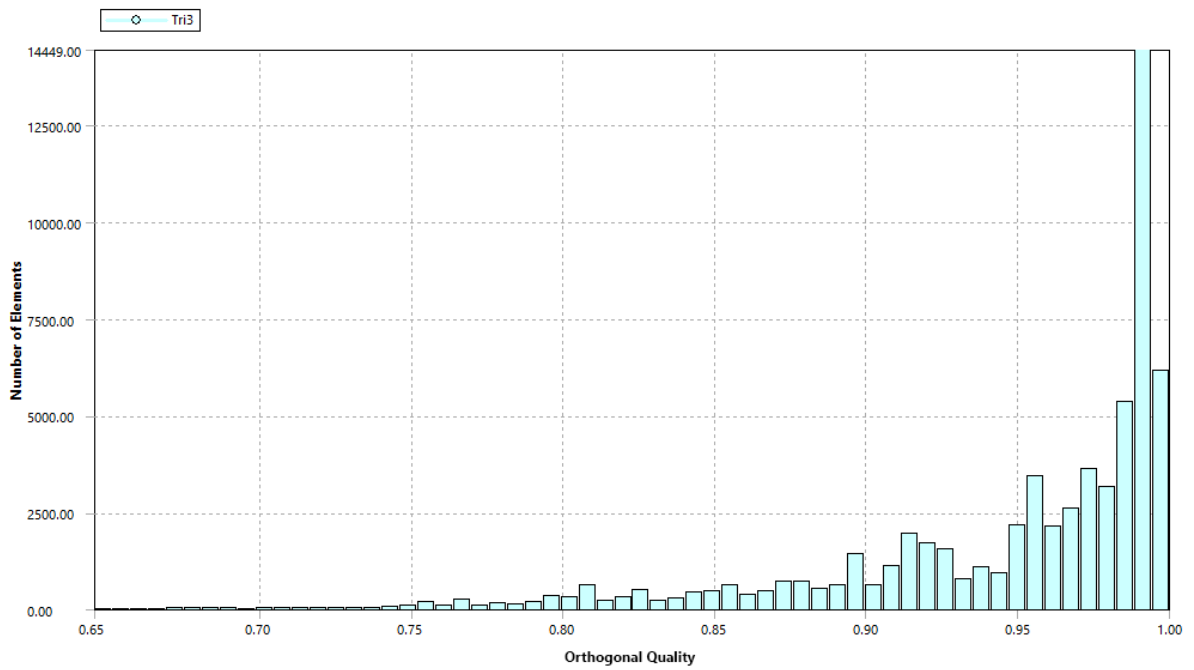


FIGURE 8: DISTRIBUTION OF ORTHOGONAL QUALITY

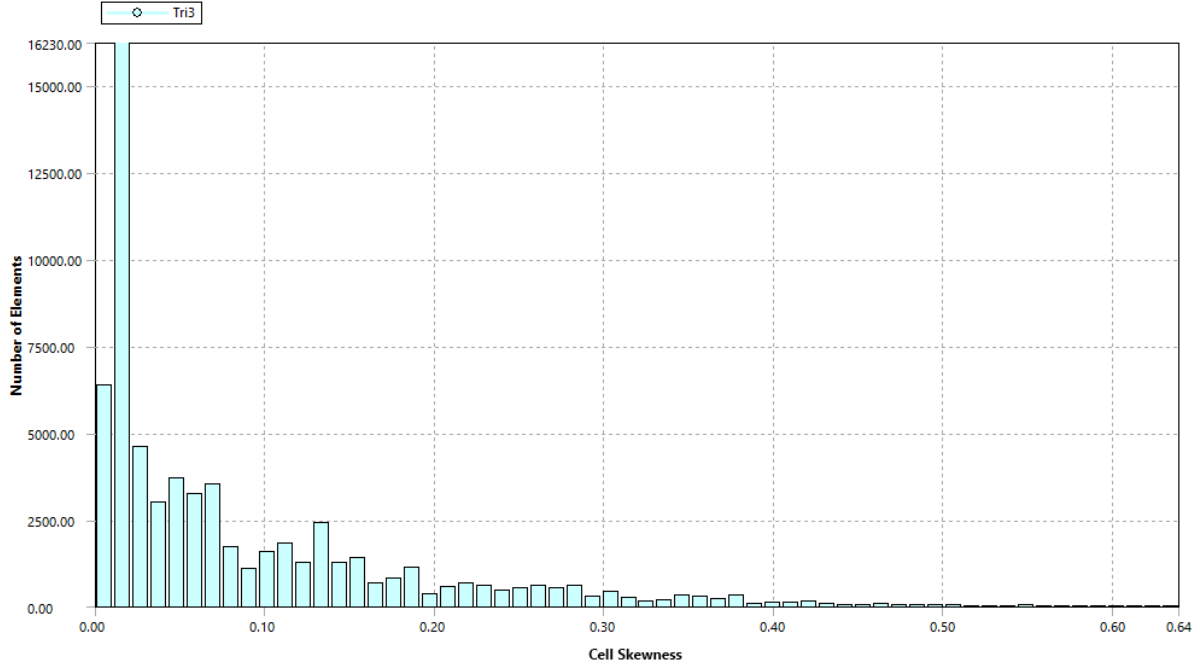


FIGURE 9: DISTRIBUTION OF CELL SKEWNESS

Boundary conditions

The boundaries were labelled as *top*, *bottom*, *inlet* and *outlet*. The boundary conditions for the *inlet* and the *outlet* boundaries were fairly straightforward. The *inlet* boundary has a Dirichlet boundary condition for pressure with the value of zero. The velocity field at the inlet boundary is initially unknown and hence, *pressure – inlet* boundary condition was incorporated. However, the *outlet* boundary cannot be described with either a Dirichlet or a Neumann boundary condition for either the velocity or the pressure fields. Hence, *outflow* boundary condition was specified for the *outlet* boundary. The *bottom* boundary is the heated wall for which the surface Nusselt number Nu_s has to be determined. Since it is the heated wall, a *wall* boundary condition with a Dirichlet boundary condition for the temperature field is used initially. The value for the Dirichlet boundary condition is determined by the value of ΔT , the temperature difference between the wall and the initial fluid temperature. Since temperature does not appear in the energy equation in its absolute terms but only as a resultant of either the ∇ operator or the ∇^2 operator, the absolute value of temperature is irrelevant. The top boundary is also given a *wall* boundary condition but is assumed as a zero-heat flux wall and is assumed to be adiabatic. Realistically, there will be an outflux of heat in the form of natural convection with surrounding air or through radiation but they are assumed to be negligible compared to the convective heat flux within the channel. Hence, the *top* wall is given a Neumann boundary condition for temperature field with a heat flux value of zero.

For the *inlet* boundary, the boundary condition used can be mathematically expressed as

$$P(x, y)|_{(x, y) \in inlet} = 0 \quad \dots (4)$$

Whereas, for the bottom boundary, the boundary condition used can be expressed as

$$T(x, y)|_{(x, y) \in bottom} = T_f|_{t=0} + \Delta T \quad \dots (5)$$

And, the boundary condition for the *top* boundary can be expressed as

$$\vec{q} = 0 = \frac{\partial T}{\partial \vec{n}} \quad \dots (6)$$

Here, \vec{n} represents the spatial parameter normal to the top boundary, which can be determined from the angle of inclination of the channel with respect to the vertical.

In real-life scenarios, the bottom boundary must be assumed not as a Dirichlet boundary condition of temperature but as a Neumann boundary condition of temperature. Since the heat outflux from the solar panel is to be made constant, the bottom boundary must be a constant heat outflux wall.

EXECUTION

Although the test case is an example of a compressible flow, the pressure-based solver and not the density-based solver is used since the flow is only mildly compressible, with the compressibility being an effect of temperature and not of pressure.

The flow is assumed to be planar unsteady flow with adequate time-stepping performed until the solution reaches a quasi-steady state. Gravity is a major external body force on the fluid and hence, an acceleration vector of 9.81 m/s² on the negative y-axis is provided. Since the flow involves variation in temperatures, the energy equation must be used to determine the temperature field. As the mode of heat transfer is natural convection, the temperature field is significant for determining buoyancy effects which are the driving force of the flow. Although the flow involves variations in the temperature field, no phase change is expected. Omitting bubble formation at the surface of the hot wall, the flow can be assumed to be single phase flow, thereby neglecting multiphase flow effects.

A characteristic feature of evaluation of the physics of natural convection is the Boussinesq approximation. Assuming the temperature variation between the inlet and the outlet to be small, the density of the convecting fluid can be assumed as a linear function of temperature as governed by the Boussinesq approximation. This simplifies the flow equations which result in a non-dimensional number characterising the flow in natural convection, the Grashof number Gr .

Solver Parameters

As mentioned above, the pressure-based solver of ANSYS Fluent was used. The SIMPLE scheme was used as the solving algorithm for pressure-velocity coupling. The gradients were discretised using the least squares cell method with pressure, momentum and energy discretised using the second order upwind method. The transient analysis was formulated using the first order implicit scheme. A standard relaxation factor of 0.75 was given to higher order terms. The under-relaxation factors for pressure and momentum were assumed to be 0.3 and 0.7 respectively with the rest of the terms, density, body forces and energy, having the default relaxation factor of 1.

The reference scales for each quantity were determined from the properties of the convecting fluid, in this case, water. The reference temperature was set as the inlet temperature of the fluid.

A standard initialisation was done before the execution of the program. The nodal values of the fields were set to the reference values, with temperature along the regime being 300K, the velocity being 0 m/s and initial pressure across the regime being 0 Pa. The residual threshold for convergence was set as 10^{-4} for velocities in both the components and the continuity while the threshold for energy was set at 10^{-6} . The convergence condition was set at all residual thresholds being met.

Time Stepping

An unsteady analysis was performed to better image the development of flow. The time step was determined using the CFL condition and adjusted based on the flow velocity in the regime. As stated by Azevedo and Sparrow, the simulation was executed for a total simulation time of 15 minutes and then extended to ensure that the flow undergoes only minor fluctuations in the values of thermophysical and flow parameters.

Variation in Parameters

The variation in the Nusselt number is a function of the angle of inclination with respect to the vertical and also the aspect ratio of the channel. This can directly be inferred from the correlation proposed by Azevedo and Sparrow. However, the correlation is only valid for inclinations up to 45° from the vertical with a tolerance of $\pm 10\%$. As the regime of focus of this article is highly inclined channels with a very low interwall spacing, the lower bound of the domain of angles considered for simulation is 79° from the vertical. Simulations were performed with variations in the angle with respect to the vertical in steps of 5° right until 75° with an additional case of 79° .

The aspect ratio as mentioned by Azevedo and Sparrow for their proposed correlation to be valid had a lower bound of 0.0437. In this article, a lower bound for the aspect ratio of 0.008 and an upper bound of 0.025 is simulated.

RESULTS AND DISCUSSION

The Nusselt number for each of the simulation cases was calculated natively in FLUENT through its Surface Integral function. The results were then tabulated in Microsoft Excel and curve fitting was performed on the simulation data.

The velocity, pressure and temperature plots were exported from FLUENT by the use of its contour feature.

Interpretation of Nusselt Number Results

To ensure that the analysis yields results of tolerable accuracy, certain benchmark cases were simulated. Azevedo and Sparrow's experiments are similar to the case in consideration and hence, the same geometry and flow conditions were simulated in order to check the validity of the results obtained.

The following table denotes the comparison between the value obtained from the correlation proposed by Azevedo and Sparrow and the values obtained through simulation in ANSYS Fluent.

Heating Mode	Angle	Aspect Ratio	Rayleigh Number	Predicted Nusselt Number	Determined Nusselt Number
Mode I	30	0.008	37212.57	2.9036	2.276676
	45				2.524641
	60				2.739123
	79				3.133041
Mode III	30	0.008	37212.57	2.6991	3.523193
	45				3.860026
	60				3.936774
	79				4.547806

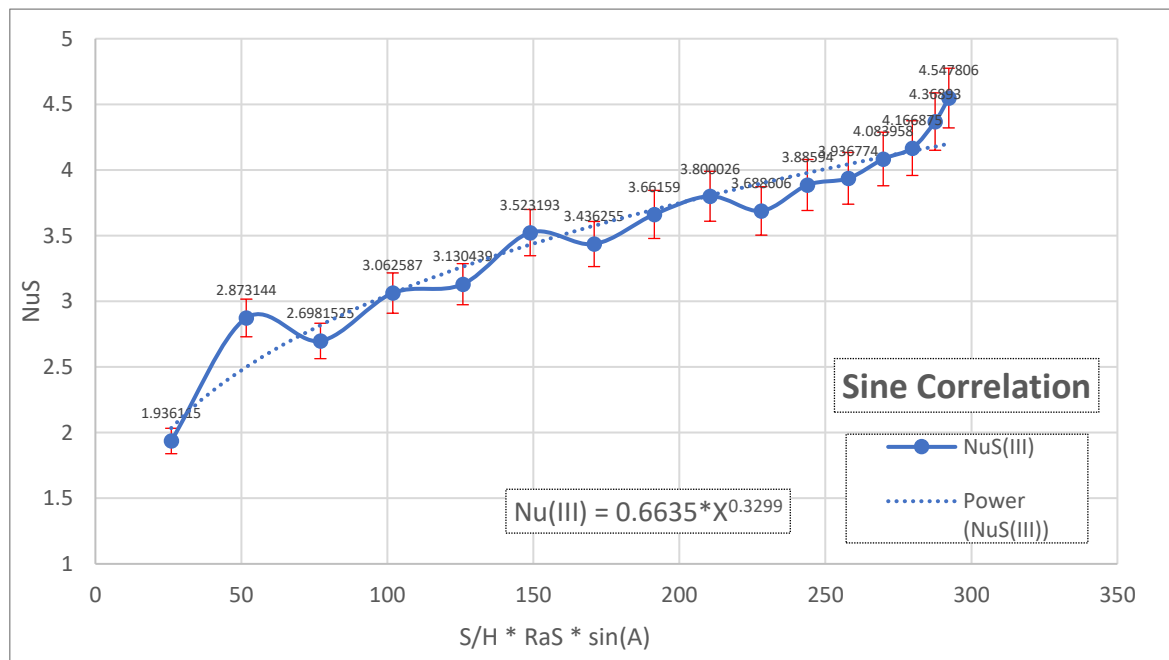
It can be seen from the table that the correlation tolerably agrees with the results from the simulation for heating mode I. However, the correlation has a stark difference for the case of heating mode III. Also noticeable from the table is the increase, and not decrease, of the Nusselt number, indicating an inverse in the relationship of the Nusselt number with the angle, from cosine at larger aspect ratios to sine at smaller aspect ratios.

This contrasting results was studied upon extensively with repeated simulations, involving smaller step sizes for heating mode III, the result of which is found in the table below:

Aspect Ratio	Angle	Rayleigh Number	$S/H * RaS * \sin(A)$	Determined Nusselt Number
0.008	5	37212.57	25.94631342	1.936115
	10		51.69515973	2.873144
	15		77.05057467	2.6981525
	20		101.8195882	3.062587
	25		125.8136932	3.130439
	30		148.85028	3.523193
	35		170.7540263	3.436255
	40		191.3582314	3.66159
	45		210.5060847	3.800026
	50		228.0518597	3.688606

Aspect Ratio	Angle	Rayleigh Number	S/H * RaS * sin(A)	Determined Nusselt Number
0.008	55	37212.57	243.8620223	3.88594
	60		257.8162477	3.936774
	65		269.8083357	4.083958
	70		279.7470194	4.166875
	75		287.5566594	4.36893
	79		292.2309622	4.547806

From the table, it can be seen that there is a vague proportionality of the Nusselt Number with the sine of the inclination angle. A simple curve fitting was done and the fitted curve was plotted against the simulation data as below.



Correlations of Nusselt Number with Parameters

The correlation of the Nusselt number with the Rayleigh number and the sine of the angle obtained is

$$Nu_S \approx 0.6635 \left(\frac{S}{H} \cdot Ra_S \cdot \sin \theta \right)^{0.33}$$

This correlation has a tolerance of $\pm 5\%$ with the data obtained from the simulation as pictured by the error bars in the figure above.

In order to investigate the change of dependence of the Nusselt number with the inclination angle from cosine to sine, another set of simulations were done with varying aspect ratios and the results of those are as follows.

Aspect Ratio	Angle	Rayleigh Number	$S/H * RaS * \sin(A)$	Predicted Nusselt Number	Determined Nusselt Number
0.01	15	72680.80078	188.1117546	3.733969	3.291784
	30		363.4040039	4.639952	4.596169
	45		513.9308709	5.201977	4.268395
	60		629.4341984	5.561791	4.737309
	75		702.0426255	5.765756	5.351681
0.015	15	245297.7026	952.3157574	6.375889	4.507061
	30		1839.73277	7.922888	5.092581
	45		2601.775034	8.882565	5.662537
	60		3186.51063	9.496961	6.735772
	75		3554.090792	9.845239	7.841275
0.02	15	581446.4063	188.1117546	9.319872	9.698949
	30		363.4040039	11.58118	6.369926
	45		513.9308709	12.98397	6.953404
	60		629.4341984	13.88206	8.303451
	75		702.0426255	14.39115	9.573449
0.025	15	1135637.512	952.3157574	12.51101	13.77878
	30		1839.73277	15.54659	7.730616
	45		2601.775034	17.4297	12.74104
	60		3186.51063	18.6353	9.469127
	75		3554.090792	19.3187	11.32551

It can be seen from the table that the correlations are tolerably valid for the aspect ratio of 0.015, however the predicted values vary drastically at values higher than the mentioned value of 0.015. Also, the determined Nusselt number seems to be increasing with the inclination angle at lower aspect ratios, indicating a correlation with the sine but as the aspect ratio increases, the values fluctuate and dictate any pattern of increase nor decrease with increasing inclination angle. This phenomenon can be scoped further and the underlying physical phenomena identified.

SUMMARY

REFERENCES